Science
AAAS

Synthetic nacre by predesigned matrix-directed mineralization

*Li-Bo Mao,[1,2] Huai-Ling Gao,[1,2] Hong-Bin Yao,[1,2] Lei Liu,[1,2,3] Helmut Cölfen,[3] Gang Liu,[4] Si-Ming Chen,[1,2] Shi-Kuo Li,[1,2] You-Xian Yan,[1,2] Yang-Yi Liu,[1,2] and Shu-Hong Yu[1,2,4]**

7 October 2016, Volume 354, Issue 6308

Debasmita Ghosh
24.06.2017

Introduction

- ✓ Biological materials are built from limited components, but their mechanical performances, such as strength and toughness, are far beyond their artificial counterparts.
- ✓ The most studied model among these biological materials is **nacre**, also called mother-of-pearl, is the iridescent material found in the interior of mollusk shells. It features a "brick-and-mortar" microstructure.
- ✓ The secret of success is their hierarchically ordered structure at multiscale levels.
- ✓ It consists of about 95 weight % (wt%) of brittle aragonitic $CaCO_3$ and 5 wt % of organic materials.
- ✓ In contrast to biological materials, the evolution of synthetic structural materials has been achieved predominately by developing new synthetic compounds rather than optimizing the micro/nanostructures of existing materials. **Therefore, bioinspired designs of multiscale structures are promising for developing surpassing structural materials.**

In this paper

- A mesoscale approach of "assembly-and-mineralization" process inspired by the natural process in mollusks to fabricate bulk synthetic nacre.
- This material highly resembles both the chemical composition and the hierarchical structure of natural nacre.
- The millimeter-thick synthetic nacre consists of alternating organic layers and aragonite platelet layers (91 weight percent) and exhibits good ultimate strength and fracture toughness.
- This predesigned matrix-directed mineralization method represents a rational strategy for the preparation of robust composite materials with hierarchically ordered structures, where various constituents are adaptable, including brittle and heat-labile materials.

Hierarchical structure of natural nacre

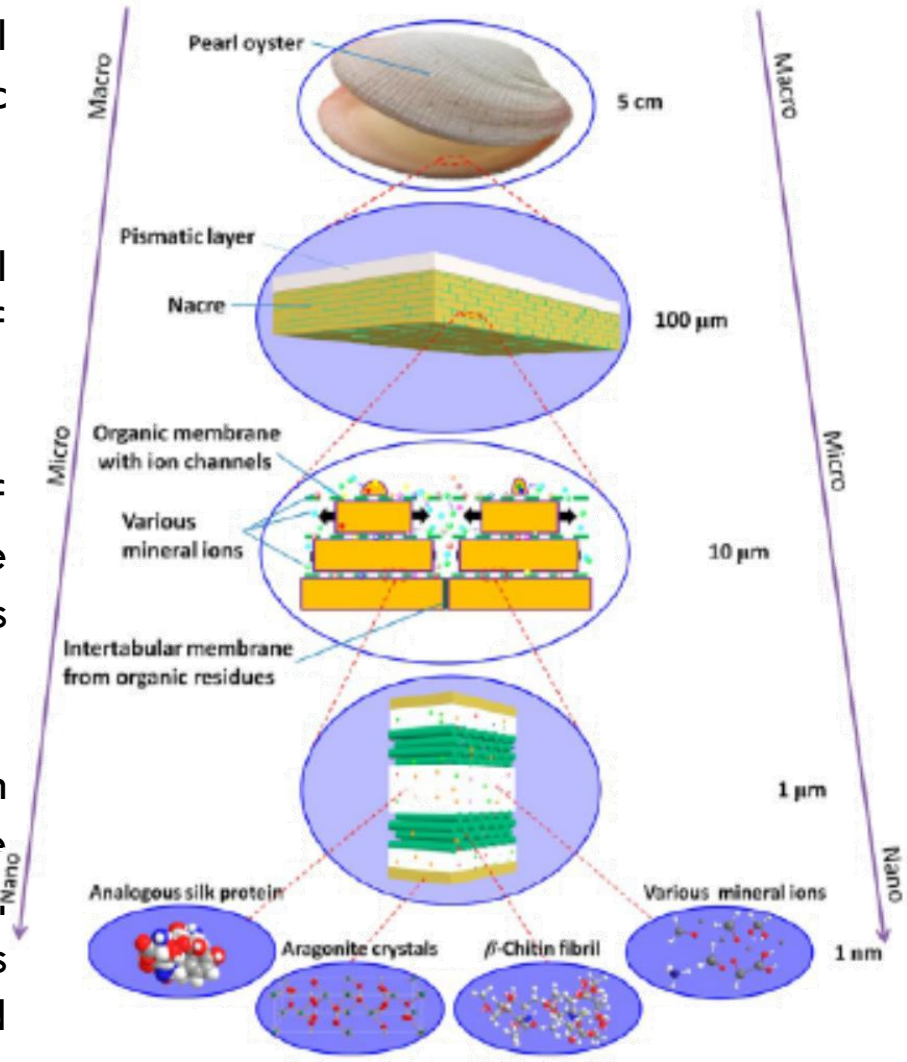

ACS Nano 2016, 10, 4816−4827

Fabrication scheme of the synthetic nacre

➢ Matrix Preparation

Chitosan (DW) —Glacial acetic acid→ Suspension (stirring) —Degassed/ ultrasonication→ Chitosan solution —4℃, Poured into PDMS mold→ frozen matrix —Dried in freeze drier treated in oven→ Dried chitosan matrix —Acetylation, Methanol/ acetic anhydride 50℃, 4h→ β-chitin

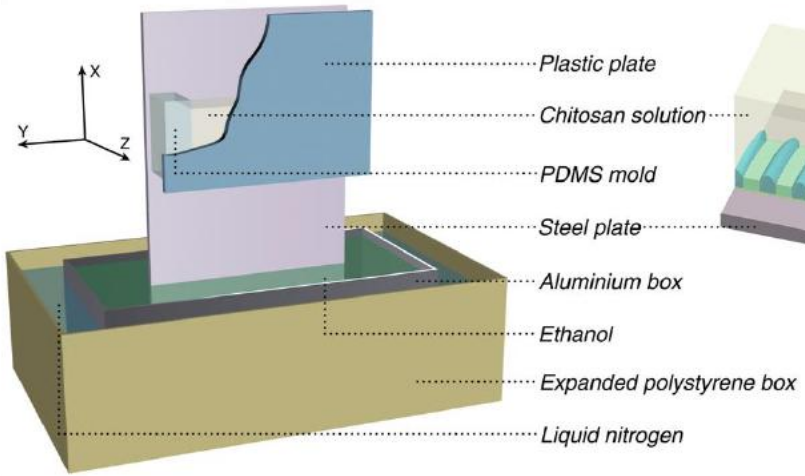

Experimental setup of the freeze-casting process

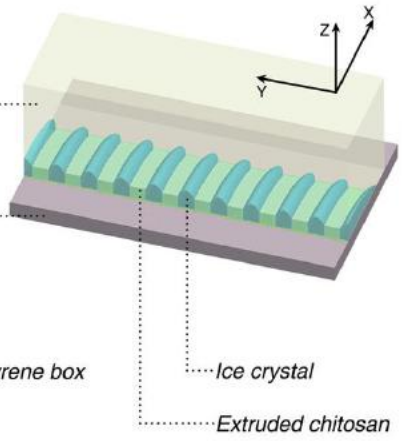

Mechanism of the formation of the laminated chitosan matrix

➢ Mineralization

$CaCO_3$ suspension (DW) —CO_2, 25℃, 45 min→ $Ca(HCO_3)_2$ —PAA, $MgCl_2$→ mineralizing solution —Pump through the matrix→ Mineralized matrix —Silk fibroin infiltration, Hot-pressing→ Laminated synthetic nacre

Fabrication scheme of the synthetic nacre

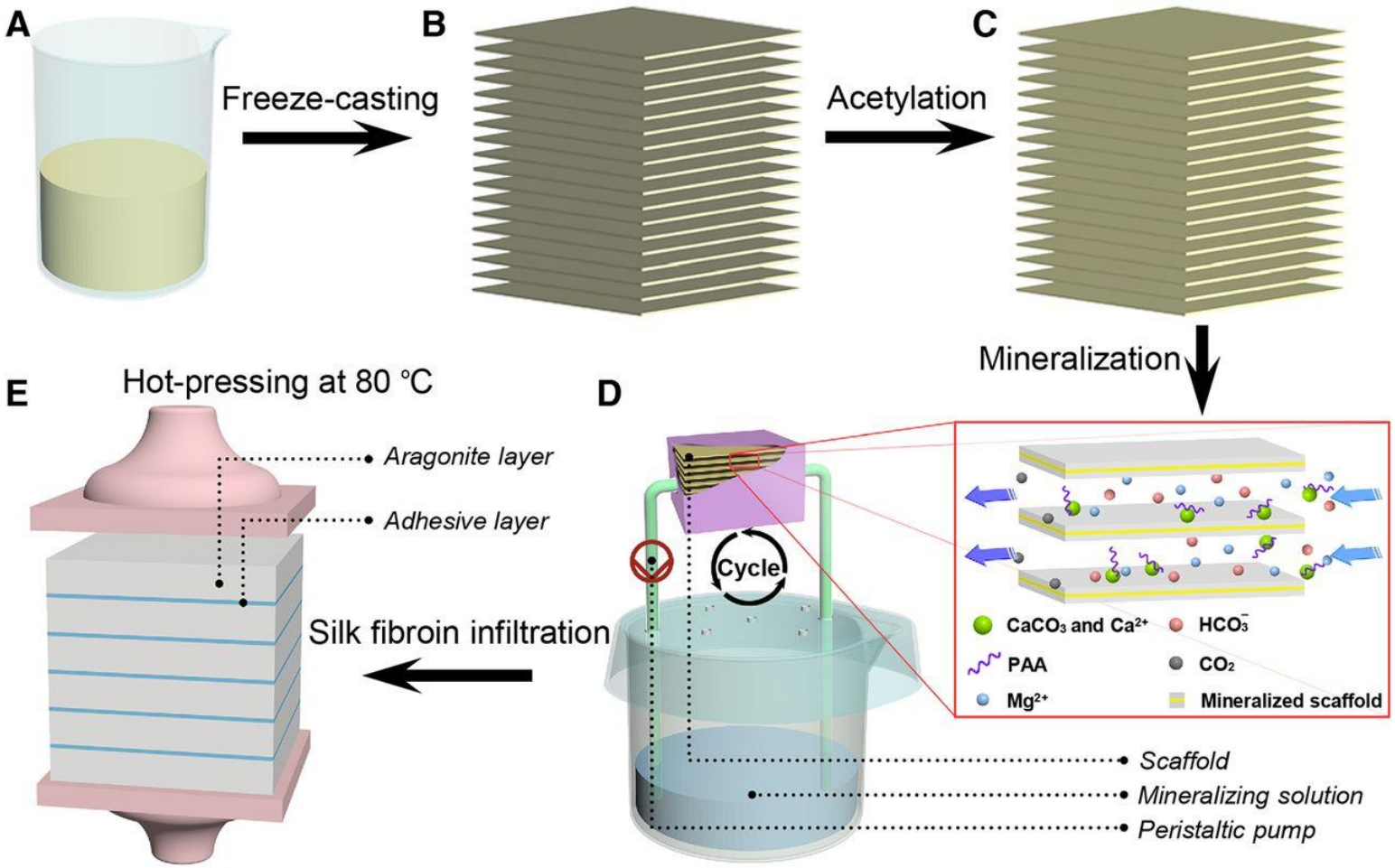

(A) Starting solution, chitosan/acetic acid solution. (B) Freeze-casted laminated chitosan matrix. (C) Matrix after acetylation where chitosan is converted to β-chitin. (D) Mineralization of the matrix. Fresh mineralizing solution is pumped to flow through the space between the layers in the matrix, bringing in Ca^{2+}, Mg^{2+}, HCO_3^- and PAA for mineralization, and taking out excess CO_2. $CaCO_3$ precipitates onto the layers and CO_2 diffuses into the air through the pin holes in the paraffin film. (E) Laminated synthetic nacre is obtained after silk fibroin-infiltration and hot-pressing.

Characterization of Acetylated and mineralized matrix

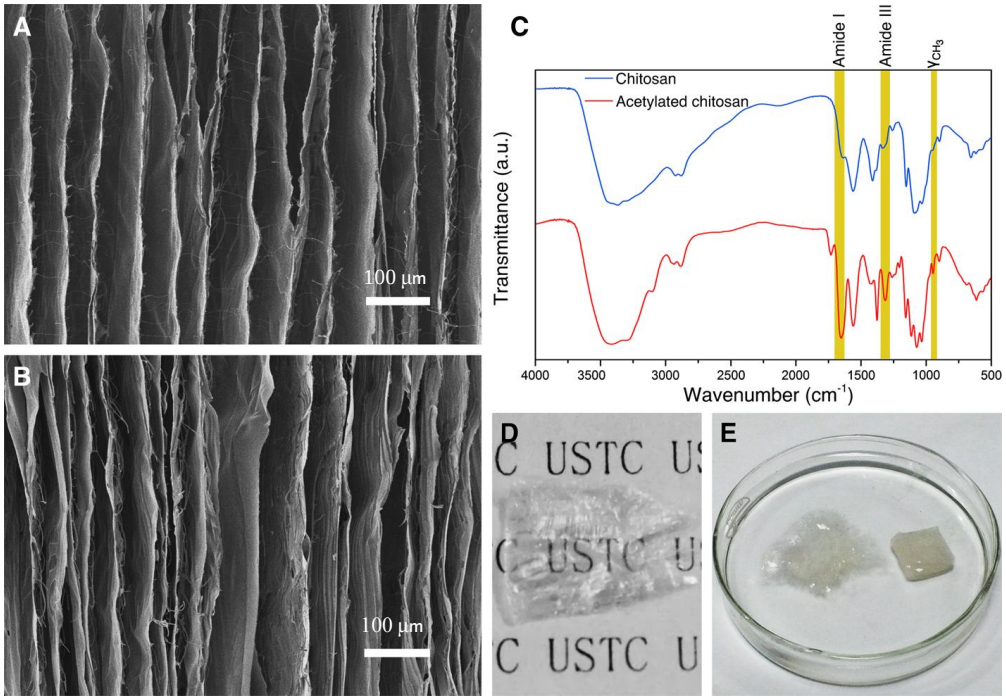

(A) Freeze-casted laminated chitosan matrix. (B)acetylated matrix.
(C) FT-IR spectrum of the matrix. (D) A transparent chitin single layer matrix.
(E) The chitosan matrix (left) and the chitin matrix (right).

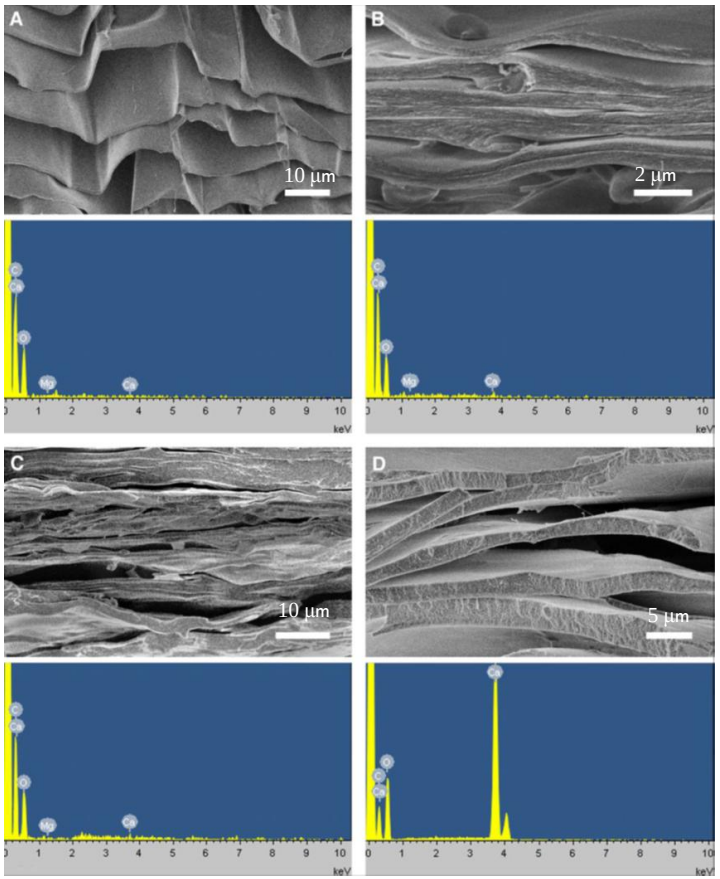

Cross sections and EDS spectra of samples fabricated by different mineralization methods (A) Compressed matrix. (B) Gas-diffusion method. (C) Soaking method. (D) Pump driven method

The comparison of the appearance and multiscale structure between natural and the synthetic nacre

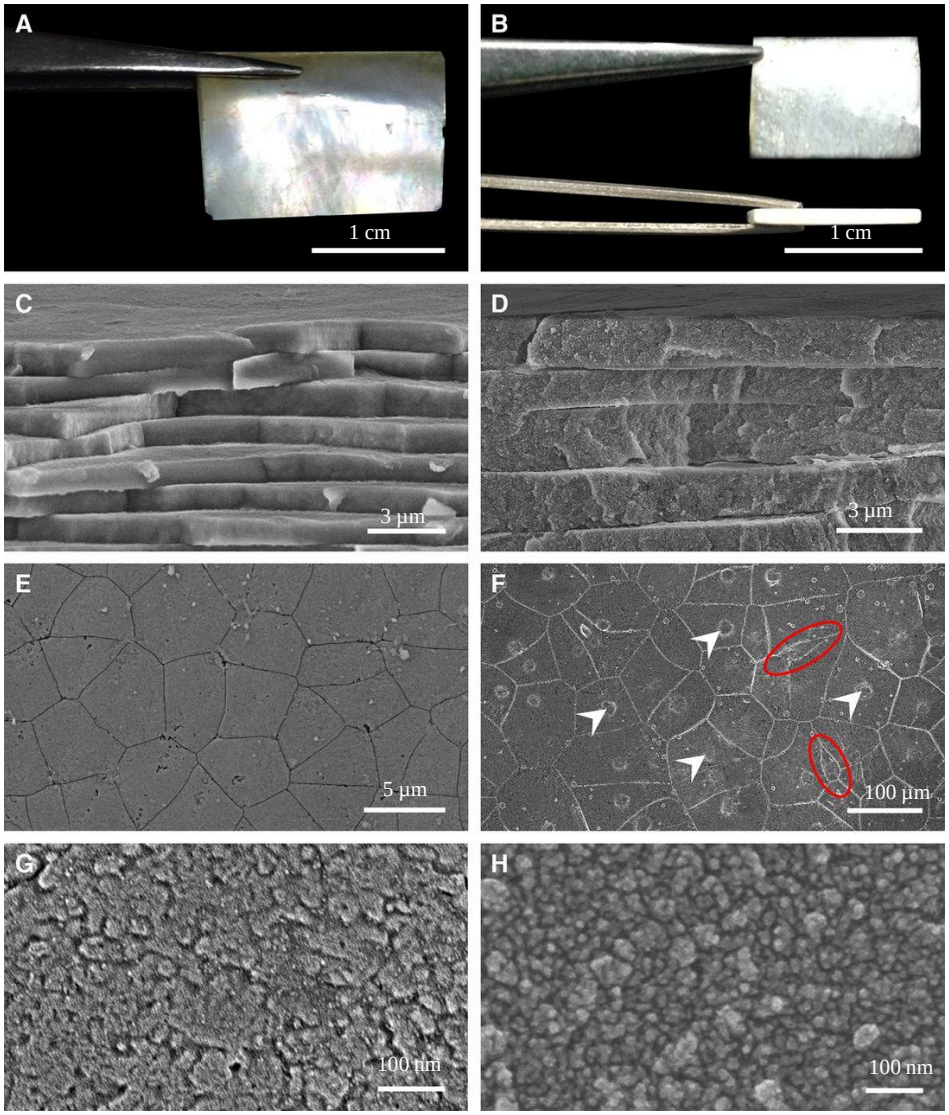

(A) *Anodonta woodiana* nacre. (B) Bulk synthetic nacre. (C and D) Fracture surface of (C) *Anodonta woodiana* nacre and (D) the synthetic nacre. (E and F) Voronoi pattern of the aragonite layer in (E) *Anodonta woodiana* nacre and (F) the synthetic nacre. (G and H) Enlarged micrographs of the aragonite platelet of (G) *Anodonta woodiana* nacre and (H) the synthetic nacre.

Micro and nano features of the synthetic nacre

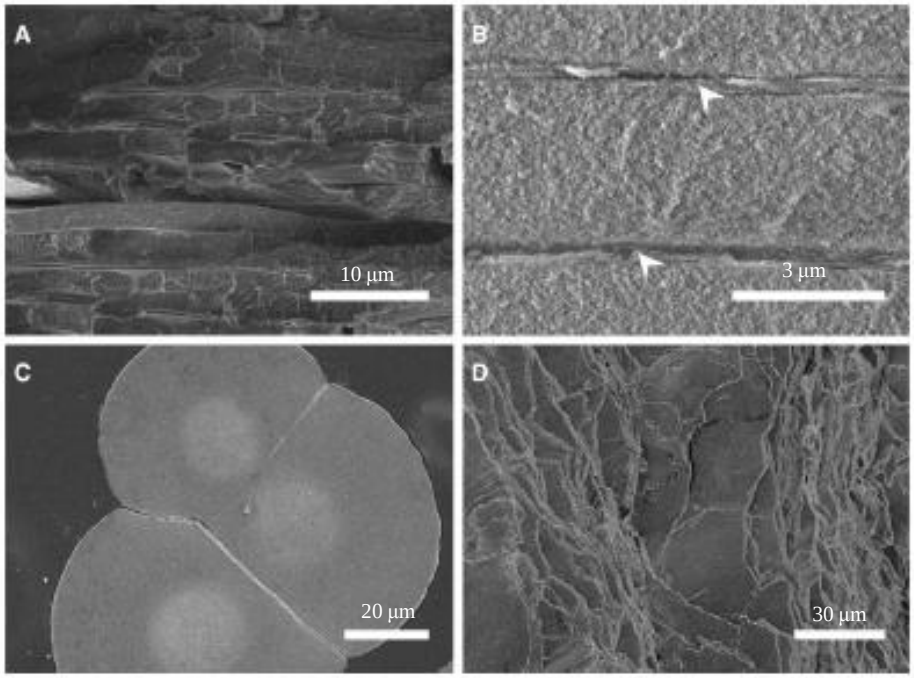

(A) Large-field-of-view laminated structure of the synthetic nacre. (B) Enlarged view of the synthetic nacre. (C) Mineralization of the chitin layer starts at separate nucleation spots similar to natural nacre. (D) Oblique view of the synthetic nacre

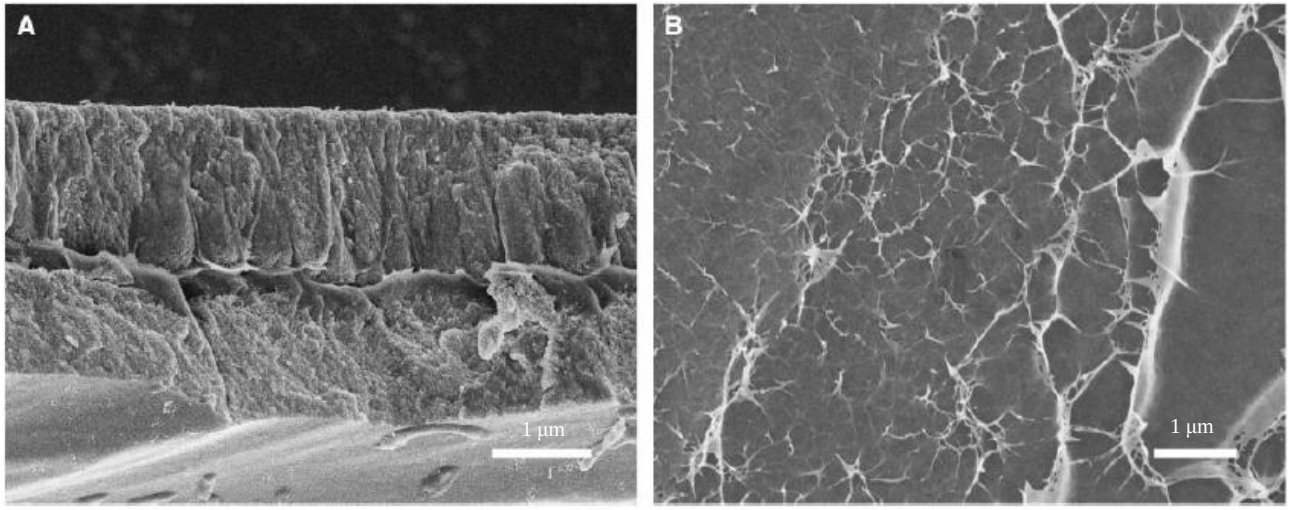

Assimilation of chitin in the synthetic nacre. (A) Mineralized layer showing chitin matrix is gradually assimilated (3 days). (B) Chitin-$CaCO_3$ interface (3 days) showing the strong interactions between them.

Crystallographic structure of the synthetic nacre

Science
AAAS

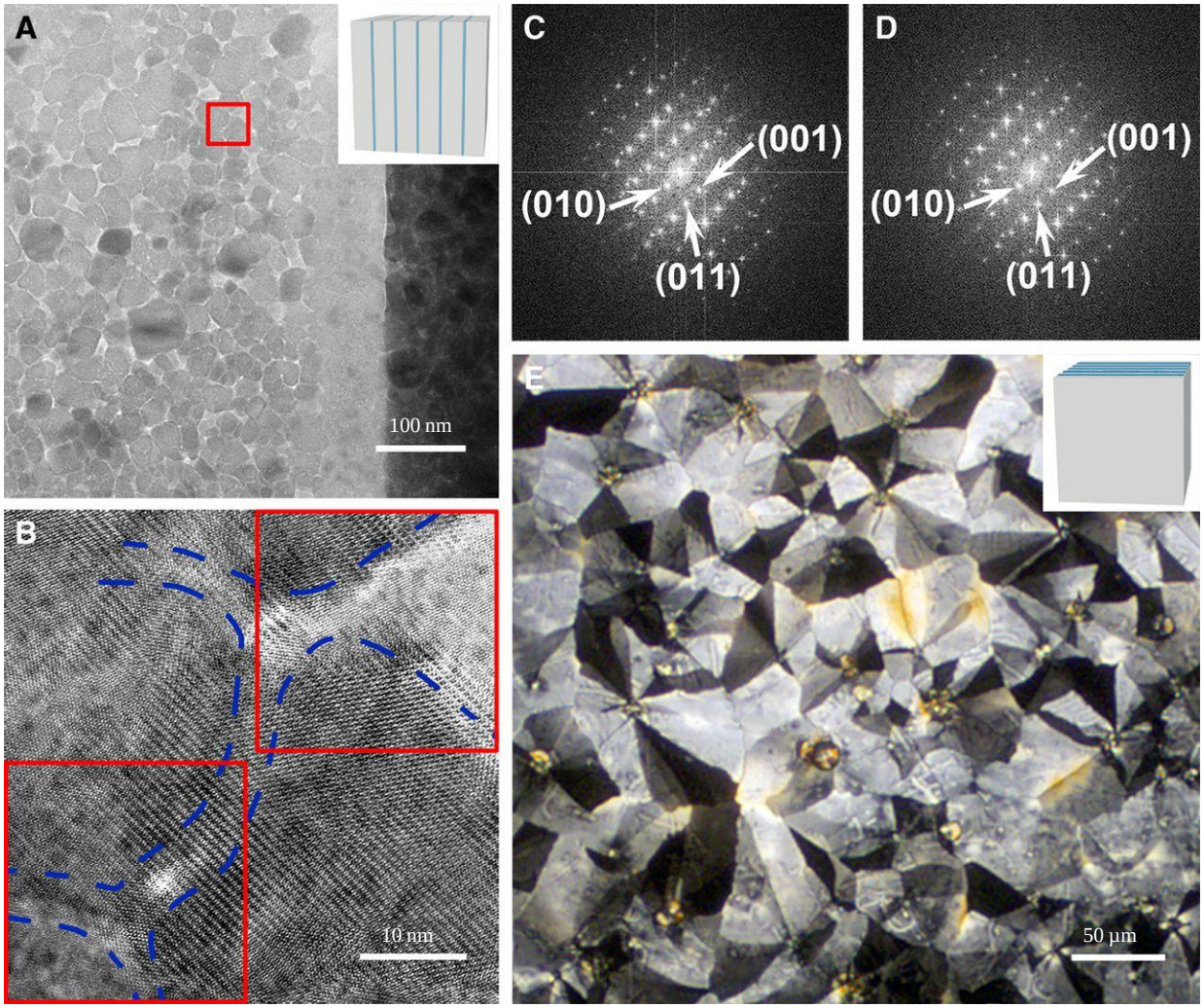

(A) Cross-sectional transmission electron microscope (TEM) image of the synthetic nacre. The inset shows the view direction. (B) High-resolution TEM (HRTEM) image of the selected area in (A). The boundaries of the nanograins are marked with dashed blue lines. (C and D) Fast Fourier transformation (FFT) of the selected squares denoted by red lines in (B), where (C) corresponds to the top right square and (D) the bottom left. (E) Optical micrograph of the aragonite layer under cross-polarized light, where the inset shows the view direction.

Statistical analysis of area distribution of the aragonite platelets

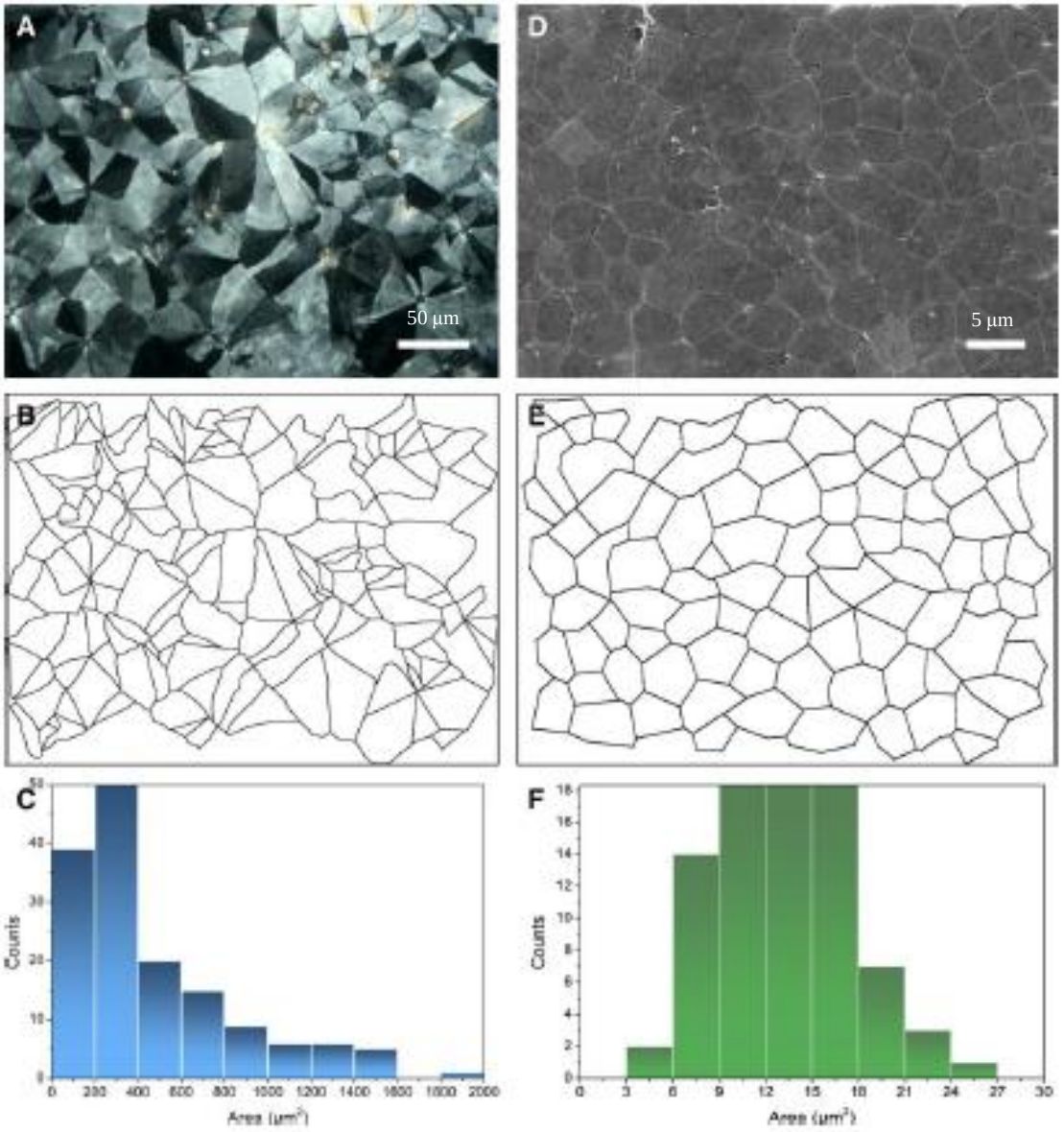

(A) Cross-polarized light micrograph of the aragonite layer in the synthetic nacre. (B) Binary image generated from (A). (C) Area distribution of platelets calculated from (B). (D) SEM micrograph of *Anodonta woodiana* nacre. (E) Binary image generated from (D). (F) Area distribution of platelets calculated from (E).

Nanoindentation test

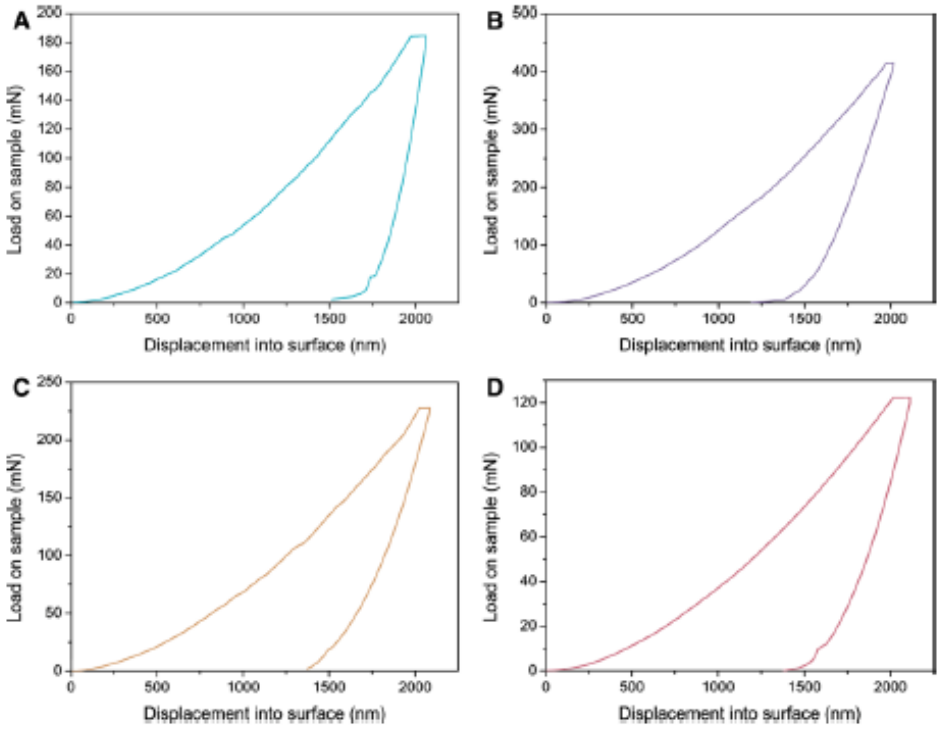

	Calcite (104)	Aragonite (001)	AW nacre (top)	Synthetic nacre (top)
Elastic modulus (GPa)	79.42 ± 0.73	109.14 ± 1.68	68.57 ± 4.48	43.39 ± 3.21
Hardness (GPa)	2.19 ± 0.05	6.77 ± 0.17	3.82 ± 0.38	1.65 ± 0.29

Load-displacement curve of (A) calcite, (B) aragonite, (C) *Anodonta woodiana* nacre and (D) the synthetic nacre. Microscopic elastic modulus and hardness data derived from the curves are listed in the table

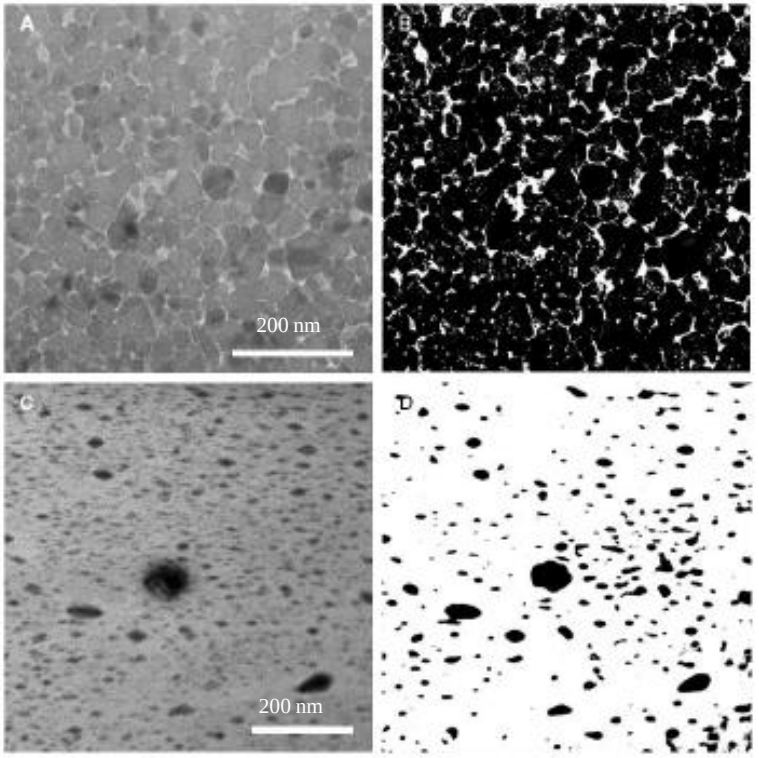

(A) Bright-field TEM image of the synthetic nacre. (B) Binary image generated from (A). (C) Dark-field TEM image of *Anodonta woodiana* nacre. (D) Binary image generated from (C).

Mechanical properties of the synthetic nacre

Science
AAAS

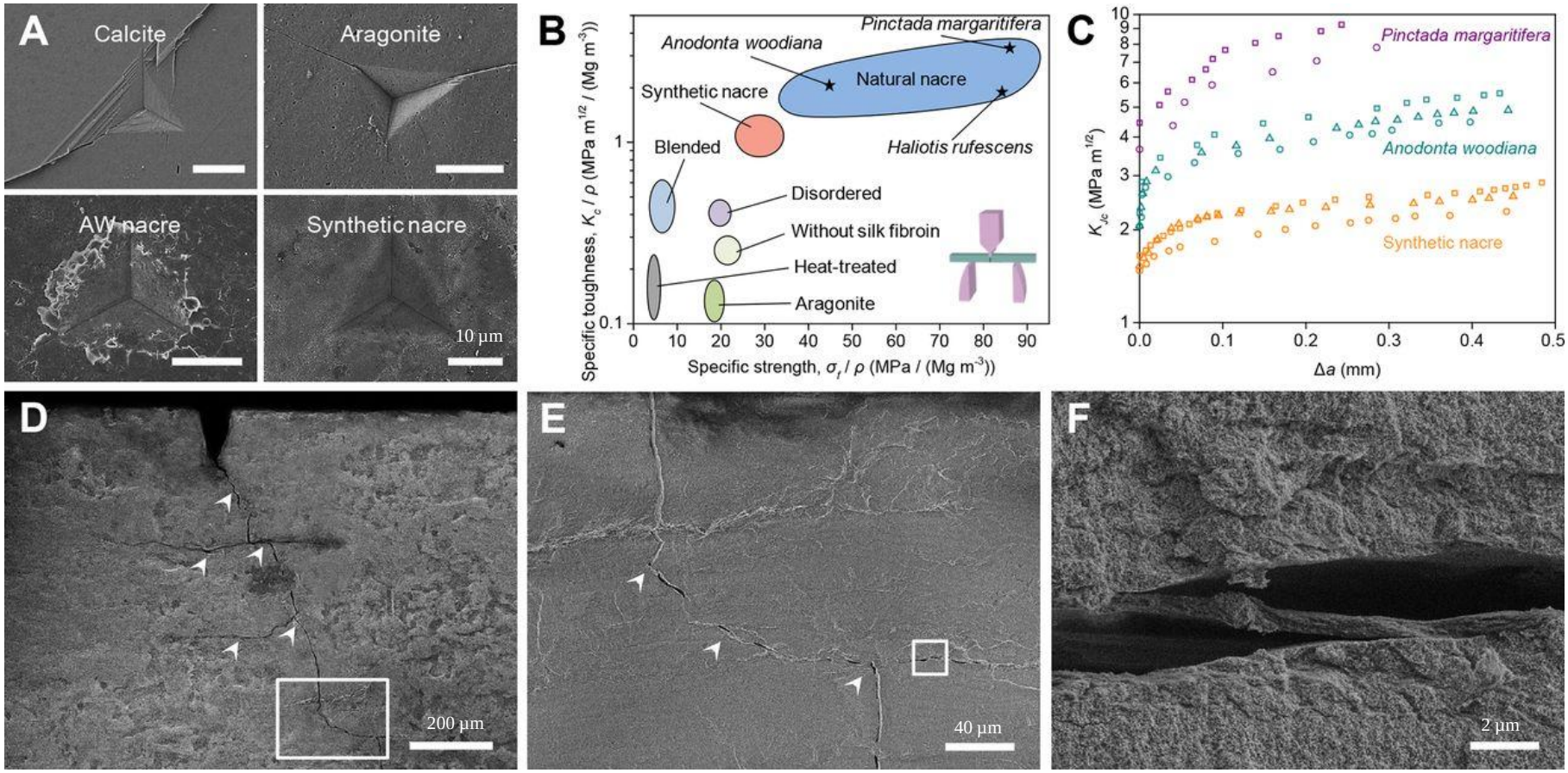

(A) Residual indents of the Berkovich diamond tip in abiotic minerals, *Anodonta woodiana* (AW) nacre and the synthetic nacre. (B) Specific fracture toughness versus specific ultimate flexural strength, illustrating the mechanical performance of the synthetic nacre, natural nacre, pure aragonite and their related materials. (C) Rising crack extension resistance curves (*K*-based) of the synthetic nacre and some natural nacre. (D) Profile of the fractured synthetic nacre showing the multiple toughening mechanisms. (E) Crack deflection between layers and crack branching [enlarged micrograph of the marked area in (D)]. (F) Crack-induced inter-lamellar debonding in the synthetic nacre (enlargement of the marked area in (E)).

Anodonta woodiana nacre and synthetic nacre under tensile stress

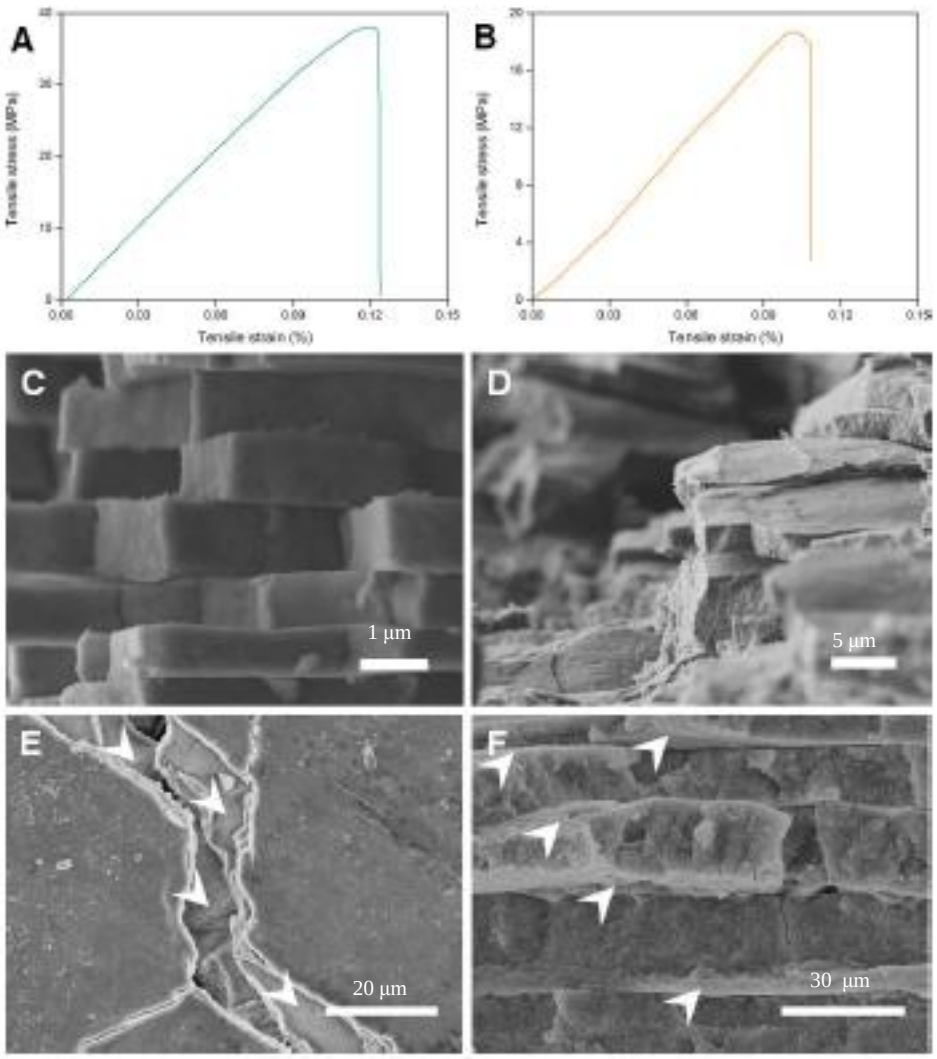

(A) Stress-strain curve of *Anodonta woodiana* nacre. (B) Stress-strain curve of the synthetic nacre. (C) Fractured surface of *Anodonta woodiana* nacre. (D) Fractured surface of the synthetic nacre. (E) Tension-induced crack of the synthetic nacre reveals the bridging of the aragonite platelets (arrows). (F) Detailed tension-induced fracture surface showing the pull-out of the platelets in the synthetic nacre (arrows).

Conclusion

- The biomimetic synthesis of nacre-like material fabricated by controlled mineralization of a multilayered organic template based on chitosan has been achieved.
- The final material is not only stiff and hard because of its high mineral content (>95% by volume) but is also surprisingly tough (it resists crack propagation and impacts).
- This level of toughness amplification has not been achieved to this day with any synthetic composite.